ChemPubSoc Europe
DOI: 10.1002/cptc.201700176
CHEMPHOTOCHEM Articles

Excited-State Pathways of Four-Coordinate N,C-Chelate Organoboron Dyes

Francisco Boscá,*[a] M. Consuelo Cuquerella,[a] Vânia F. Pais,[b, c] Abel Ros,[d, e] and Uwe Pischel*[b]

The excited-state behavior of four-coordinate N,C-chelate organoboron dyes, based on arylisoquinoline ligands with varying degree of charge-transfer character, was characterized. Data related to excited triplet state formation, oxygen quenching, and singlet-oxygen formation were obtained. The results jointly rationalize the previously observed high photostability of the dyes in air-equilibrated media. Furthermore, femtosecond transient absorption experiments enabled the spectroscopic visualization of the excited intramolecular charge transfer (ICT) state that gives rise to the fluorescence of the dyes.

1. Introduction

Over the last ten to fifteen years organoboron architectures have drawn elevated attention, not only for their interesting and versatile structural chemistry, but very often for their appealing photophysical properties. In this context the interest in new organoboron compounds as fluorescent dye platforms is steadily growing with the aim to optimize and diversify photophysical and photochemical properties, such as light absorption, emission quantum yields, or photochemical stability. Three-coordinate organoboron dyes[1,2] contain electron-deficient boron. This electronic feature introduces acceptor properties that may be integrated in sophisticated charge-transfer architectures[3–7] and two-photon-addressable molecules.[8,9] The Lewis acidic nature of trivalent boron can be used for the design of chemosensors for fluoride.[10–14] More recently, three-coordinate organoboron dyes have been also employed for bioimaging.[15] Four-coordinate organoboron dyes with chelate ligands, containing N- and/or O-donor atoms, are of elevated interest for the development of optoelectronic devices, such as organic light emitting diodes,[16,17] as photoaddressable materials,[18–20] and very frequently as dyes for bioimaging and sensing.[21–45]

As part of our research program we have been interested in arylisoquinolines as chelate ligands for organoboron dyes (BAI dyes) with specific focus on their appropriateness for bioimaging with confocal or multiphoton fluorescence microscopy.[46–48] In a recent work we have demonstrated that four-coordinate N,C-chelate dyes such as the ones shown in Figure 1 (dye **1**–**4**) are interesting candidates for these applications.[47] The dyes show high fluorescence quantum yields (up to 0.8) and, related to their intramolecular charge-transfer (ICT) character, large Stokes shifts (circa 3000–5000 cm^{-1}) and pronounced solvatochromic effects (difference of dipole moment between ground

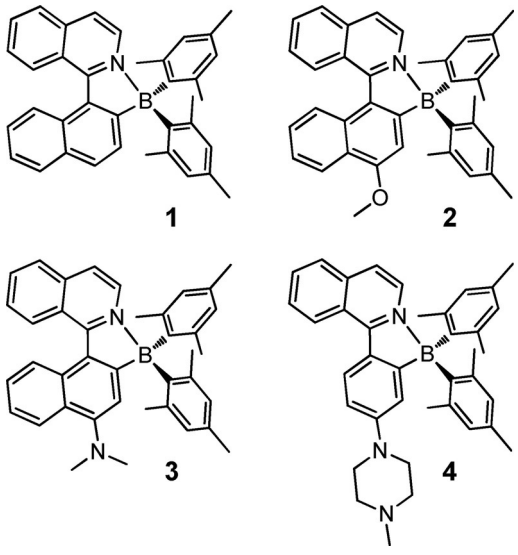

Figure 1. Structures of the dyes **1**–**4** (formal charges are omitted for simplicity).

[a] *Dr. F. Boscá, Dr. M. C. Cuquerella*
Instituto Universitario Mixto de Tecnología Química (ITQ-UPV)
Universitat Politècnica de València
Av. de los Naranjos s/n, 46022 Valencia (Spain)
E-mail: fbosca@itq.upv.es

[b] *Dr. V. F. Pais, Dr. U. Pischel*
CIQSO—Center for Research in Sustainable Chemistry and
Department of Chemistry
University of Huelva
Campus de El Carmen s/n, 21071 Huelva (Spain)
E-mail: uwe.pischel@diq.uhu.es

[c] *Dr. V. F. Pais*
Laboratório Associado para a Química Verde (LAQV)
Rede de Química e Tecnologia (REQUIMTE) and Departamento de Química
Faculdade de Ciências e Tecnologia
Universidade NOVA de Lisboa
2829-516 Caparica (Portugal)

[d] *Dr. A. Ros*
Instituto de Investigaciones Químicas (IIQ, CSIC-US)
C/Américo Vespucio 49, 41092 Sevilla (Spain)

[e] *Dr. A. Ros*
Departamento de Química Orgánica
Centro de Innovación en Química Avanzada (ORFEO-CINQA)
Universidad de Sevilla
C/Prof. García González 1, 41012 Sevilla (Spain)

The ORCID identification number(s) for the author(s) of this article can be found under: https://doi.org/10.1002/cptc.201700176.

© 2018 Wiley-VCH Verlag GmbH & Co. KGaA, Weinheim

and excited state of circa 16 D for dye **3**).[47] Additional observations indicated a desired high photochemical stability. In the present work we aimed at a more complete understanding of the excited-state processes of these dyes. For this purpose, laser flash photolysis studies with femto- and nanosecond time resolution in conjunction with classical fluorescence quenching studies were performed. This provided valuable insights into the role of oxygen quenching, triplet-state formation, and singlet-oxygen formation. These aspects in particular would appear to be closely related to the photostability of dyes.

2. Results and Discussion

2.1. Excited Singlet States of the Dyes 1–4

Following the logical order of the well-known Jablonski diagram, the photophysical description (see key data in Table 1) of the herein investigated organoboron dyes **1**–**4** (Figure 1) starts with the characterization of their excited singlet states. The fluorescence lifetimes (τ_{fluo}) and quantum yields (Φ_{fluo}) were determined in polar acetonitrile and compared with those obtained previously in nonpolar toluene,[47] both under aerobic and anaerobic conditions.

Table 1. Photophysical properties of the N,C-chelate organoboron dyes **1**–**4** in acetonitrile and toluene.

Property	1	2	3	4
Acetonitrile				
λ_{fluo} [nm][a]	492	497	577	527
λ_{T-T} [nm][b]	630	630	630	640
τ_{fluo} [ns][c]	9.5	10.3	11.3	0.6
Φ_{fluo}[d]	0.42 (0.33)	0.80 (0.64)	0.58 (0.48)	0.05 (0.05)
k_r [s^{-1}][e]	4.4×10^7	7.8×10^7	5.1×10^7	8.3×10^7
k_{nr} [s^{-1}][f]	2.4×10^7	1.5×10^7	3.5×10^7	1.6×10^9[g]
τ_T [µs][h]	8	42	37	47
Φ_{ISC}[i]	0.35 (0.32)	0.05 (0.05)	0.03 (0.03)	–
k_{ISC} [s^{-1}][j]	3.7×10^7	4.9×10^6	2.7×10^6	–
Toluene				
λ_{fluo} [nm][a]	486	492	547	506
λ_{phos} [nm][k]	570	580	620	570
λ_{T-T} [nm][b]	640	640	650	650
τ_{fluo} [ns][c]	6.2	8.6	7.7	5.0
Φ_{fluo}[d]	0.40 (0.35)	0.70 (0.62)	0.73 (0.52)	0.52 (0.44)
k_r [s^{-1}][e]	6.5×10^7	8.1×10^7	9.5×10^7	1.0×10^8
k_{nr} [s^{-1}][f]	4.8×10^7	2.9×10^7	3.1×10^7	8.6×10^7
τ_T [µs][h]	18	24	30	30
Φ_{ISC}[i]	0.30 (0.32)	0.05 (0.10)	<0.03 (0.11)	0.05 (0.16)
k_{ISC} [s^{-1}][j]	4.8×10^7	5.8×10^6	$<3.9\times10^6$	1.0×10^7
Φ_Δ[l]	0.34	0.09	0.09	0.08

[a] Fluorescence maximum, aerated solution. [b] Maximum of triplet–triplet transient absorption. [c] Fluorescence lifetime, N_2-saturated solution. The values for toluene are in accordance with Ref. [47]. [d] Fluorescence quantum yield in N_2-saturated solution; in parentheses the corresponding values for aerated solutions are given. The values for toluene are in accordance with Ref. [47]. [e] Radiative decay rate constant. [f] Non-radiative decay rate constant. [g] Corresponds to the rate constant of intramolecular photoinduced electron transfer. [h] Triplet lifetime, N_2-saturated solution. [i] Intersystem crossing (ISC) quantum yield in N_2-saturated solution; in parentheses the corresponding values for aerated solutions are given. [j] Intersystem crossing (ISC) rate constant. [k] Phosphorescence maximum. [l] Singlet-oxygen quantum yield.

The fluorescence lifetimes of the dyes **1**–**3** under nitrogen atmosphere are about 9.5–11.3 ns in acetonitrile and 6.2–8.6 ns in toluene. However, dye **4** behaves different in showing a very short fluorescence lifetime in acetonitrile (circa 600 ps). In toluene the lifetime of **4** is comparable to that of the other dyes, being only somewhat smaller (5.0 ns). The fluorescence quantum yields follow a similar trend as the lifetimes, being highest for the dyes **2** and **3** both in acetonitrile and toluene, reaching up to 0.8 for dye **2**. The radiative (k_r) and non-radiative (k_{nr}, not accounting for ISC; see the Experimental Section) decay rate constants are very comparable for the different investigated dyes (10^7–10^8 s^{-1} both in acetonitrile and toluene; see Table 1), except for dye **4** (see below). Thus, the differences in the fluorescence quantum yield, especially the lower Φ_{fluo} of **1** as compared to dyes **2** an **3**, are mainly related to the more efficient intersystem crossing (ISC) in **1** (see below).

In accordance with the previously proposed[47] intramolecular photoinduced electron transfer (IPET) from the distant amino N atom of the piperazine unit of dye **4** in polar solvents (see Scheme 1), the fluorescence quantum yield for this dye drops to 0.05 in acetonitrile. This corresponds to 90% quenching with respect to toluene as nonpolar medium and parallels the observations that were made for the lifetimes (see above). Assuming that the IPET is the only decay pathway that competes with the fluorescence, an unimolecular rate constant of $k_{IPET}=1.6\times10^9$ s^{-1} can be calculated. This agrees reasonably with the decay time of the ICT state, determined by femtosecond transient spectroscopy (350 ps; see below) in acetonitrile.

The fluorescence lifetime of the dyes **1**–**3** in acetonitrile is only moderately quenched by oxygen (circa 20% quenching at 1.7×10^{-3} M oxygen in aerated solution), while the excited singlet state of **4** is too short-lived for showing significant bimolecular quenching at millimolar oxygen concentration. The quenching is paralleled by the observations made for the fluorescence quantum yields. This points to a purely dynamic quenching with bimolecular rate constants between $0.9\times$

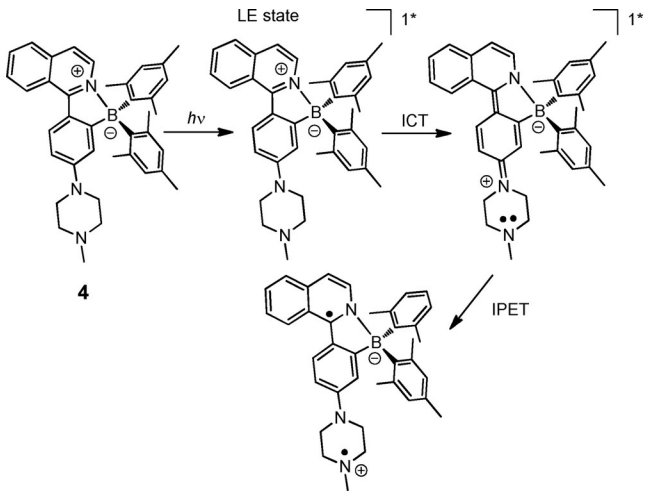

Scheme 1. Photophysical processes of dye **4** in polar solvents (e.g., acetonitrile); LE: locally-excited, ICT: intramolecular charge transfer, IPET: intramolecular photoinduced electron transfer.

© 2018 Wiley-VCH Verlag GmbH & Co. KGaA, Weinheim

$10^{10}\,M^{-1}s^{-1}$ and $1.4\times10^{10}\,M^{-1}s^{-1}$, coinciding practically with the diffusion-controlled limit ($k_{diff}=1.9\times10^{10}\,M^{-1}s^{-1}$).

In aerated toluene the fluorescence of all four dyes is quenched to a very similar extent as observed for acetonitrile (see Figure 2 for the representative example of dye **3**). However, both static and dynamic quenching apply in the nonpolar solvent. With the dynamic quenching rate constant, as derived

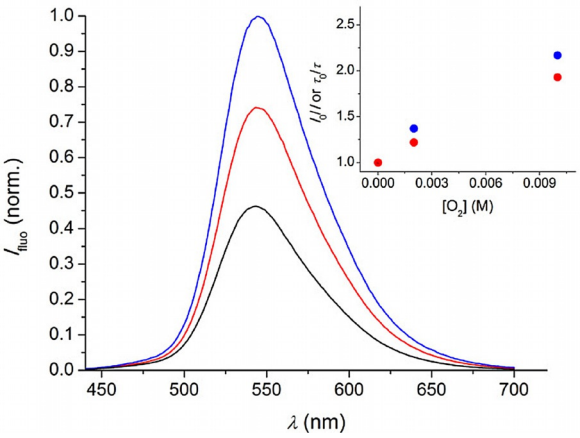

Figure 2. Fluorescence quenching of **3** by oxygen in toluene (blue line = N_2-saturated solution, red = aerated solution, black = O_2-saturated solution). The inset shows the Stern–Volmer plots for the lifetime quenching (red data points) and the intensity quenching (blue data points).

from the lifetime quenching experiments, the association constants (K_a) between the organoboron dyes and oxygen were determined as $<10\,M^{-1}$ for **1** and **2** and $100\,M^{-1}$ and $30\,M^{-1}$ for **3** and **4**, respectively (see the Experimental Section). Thus, the presence of electron-donating amino substituents at the aryl residue seems to favor the interaction with oxygen. This could be ascribed to the formation of a contact ground-state complex with oxygen as electron acceptor. Although oxygen quenching of the dyes plays a role for its excited state behavior, the absolute quenching effects are only moderate due to the rather short excited singlet-state lifetimes.

In order to gain further insight into the nature of the excited singlet state of the organoboron dye **4**, the one with the most peculiar behavior due to the occurrence of an IPET, femtosecond transient absorption spectroscopy was performed. In aerated acetonitrile two intermediates with different kinetics were observed (Figure 3). Beside the expected stimulated emission, seen as a negative signal, two transients with lifetimes of circa 1 ps and circa 350 ps were detected. The time constant of the formation of the longer-lived transient corresponds with the decay of the short-lived transient (Figure 3b). Further, the decay of the long-lived transient correlates with the disappearance of the stimulated emission (Figure 3c and Figure 3d). Thus, the transients were assigned to the S_1–S_n absorption of: a) the short-lived locally-excited (LE) singlet state and b) the longer-lived excited-singlet ICT state. The latter can be clearly related to the signal at 475 nm. Note that the very short lifetime of the LE state allows the individual observation of the ICT state at 10 ps time delay. The assignment of the spectral

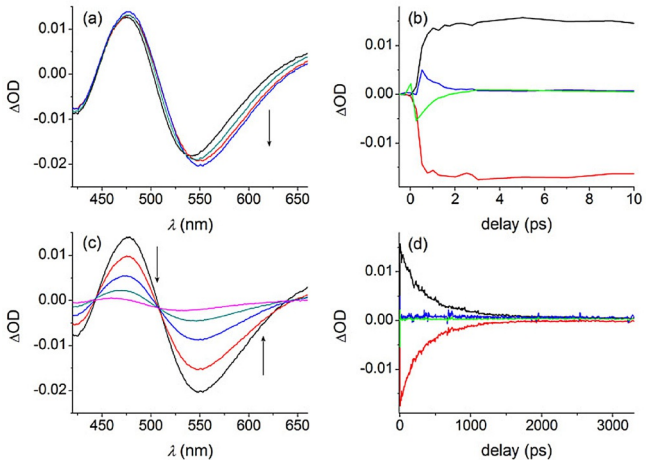

Figure 3. Femtosecond transient absorption spectra and kinetics of **4** in aerated acetonitrile ($\lambda_{exc}=350$ nm). a) Spectra with time delays of 2–8 ps. b) Kinetics in the time window 0–10 ps; probe wavelength: black line = 478 nm, blue = 639 nm, green = 508 nm, red = 539 nm. c) Spectra with time delays of 10 ps–1 ns. d) Kinetics in the time window 0–3.4 ns; same color-coding as in (b).

signal of the LE state is more difficult as it coincides with the negative signal of the stimulated emission at >500 nm. In accordance, in the course of the decay of the LE state a red-shift of the stimulated emission signal was observed (Figure 3a). The transient spectra of **4** in aerated toluene are similar. However, the lifetimes of both intermediates are longer, i.e., circa 5 ps for the first and >3 ns for the second transient.

2.2. Excited Triplet States of the Dyes 1–4

Nanosecond laser flash photolysis ($\lambda_{exc}=355$ nm) of N_2-saturated acetonitrile solutions led to transient absorption spectra with a main band maximum between 630 and 650 nm for the dyes **1**–**3** (see spectrum of **1** in Figure 4a). For dye **4** no clear band maximum, but a rather broad and weak signal was detected (Figure 4b). Interestingly, the transient absorption band of **1** is three times more intense than those detected for the other dyes, pointing to a more efficient intersystem crossing (ISC; see below). The presence of oxygen produced an efficient quenching of the transients with a rate constant ($k_q(O_2)\approx2\times10^9\,M^{-1}s^{-1}$) that is just one order of magnitude below the diffusion-controlled rate limit. When the same study was performed using toluene under anaerobic conditions, the transient absorption spectra of **1**–**4** and the associated observations were very similar to those made for **1**–**3** in acetonitrile. This fact, the lifetime in the microsecond range, and the efficient quenching by oxygen suggest the assignation of these transient species to excited triplet states, except for dye **4** in acetonitrile where the IPET is responsible for 90% of the deactivation of the excited singlet state (see above). The weak transient that was seen for dye **4** (Figure 4b) in acetonitrile is tentatively assigned to a transient that results from IPET.

The assignation to excited triplet states is corroborated by the implementation of an energy-transfer reaction between the transient and an energy-acceptor molecule. In order to

© 2018 Wiley-VCH Verlag GmbH & Co. KGaA, Weinheim

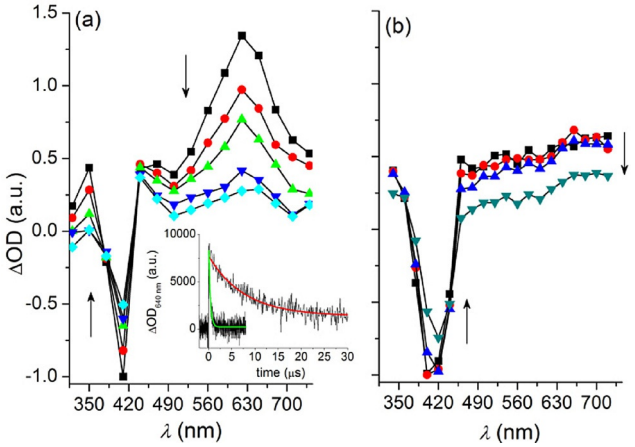

Figure 4. Transient absorption spectra of a) **1** (time window: 2–30 μs) and b) **4** (time window: 0.6–30 μs) in N_2-saturated acetonitrile (λ_{exc} = 355 nm). Inset: Kinetics of the decay at 640 nm for dye **1** in N_2-saturated solution (red) and aerated solution (green).

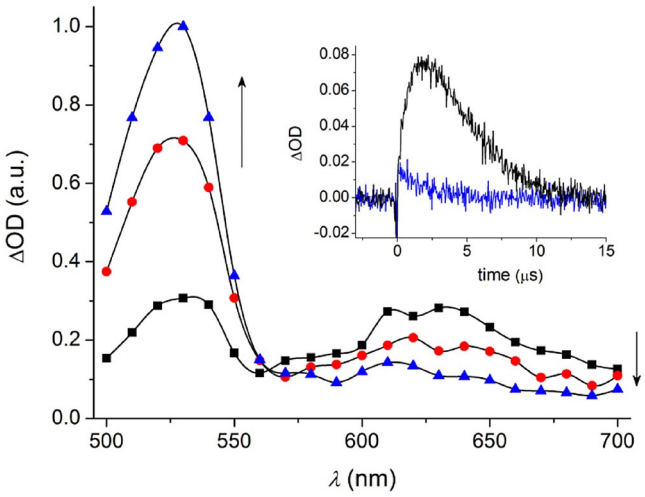

Figure 5. Transient absorption spectra for a mixture of **1** and β-C in N_2-saturated toluene; λ_{exc} = 355 nm, time window = 0.16–1.5 μs. Inset: The corresponding kinetics at 530 nm (black) and 650 nm (blue).

assure a downhill triplet energy transfer with a purposefully selected energy acceptor, the triplet energies of **1**–**4** were determined. Phosphorescence measurements at 77 K were performed on solutions of **1**–**4** in toluene and energies of 2.2, 2.2, 2.1, and 2.3 eV, respectively, were obtained from the high-energy onset of the phosphorescence emission spectrum. Thus, β-carotene (β-C) was chosen as energy acceptor because its excited triplet state (^{3}β-C*) has an energy of 0.8 eV.[49] Importantly, it is not problematic that ^{3}β-C* is also absorbing at the excitation wavelength (355 nm) of **1**–**4** because the direct population of ^{3}β-C* through intersystem crossing (ISC) is practically negligible.[50]

When solutions of **1**–**4** in toluene were submitted to laser flash photolysis at 355 nm excitation in the presence of varying concentrations of β-C, a shorter decay at 640 nm was observed. Moreover, the decay at 640 nm of the intermediates of **1**–**4** is accompanied by the concomitant growth of a new signal at 525 nm, corresponding to the triplet–triplet absorption of ^{3}β-C* (see Figure 5).[51] This experiment points to an efficient triplet energy transfer (estimated as k_{ET} circa 3×10^9 $M^{-1}s^{-1}$ for ^{3}**1*** as energy donor) and forms the basis for the determination of the molar absorption coefficient of ^{3}**1*** (see the Experimental Section). A value of $11\,200\pm1050$ M^{-1} cm^{-1} at 640 nm in toluene solution resulted. Then the intersystem crossing quantum yields (Φ_{ISC}) of the dyes **1**–**4** in toluene and acetonitrile were determined by a relative method, comparing the signal amplitudes of the triplet–triplet absorption signal of optically matched solutions of benzophenone (BP) and **1**–**4** (see the Experimental Section). The corresponding results are shown in Table 1, corroborating quantitatively the efficient ISC for **1** and much less efficient ISC for **2**–**4**. In total agreement, the calculated ISC rate constant (k_{ISC}) is about one order of magnitude faster for **1** (10^7 s^{-1}) as compared to the dyes **2**–**4** (10^6 s^{-1}). This confirms the notion that ICT states often work as an "energy sink" from where the access to other excited-state pathways, for example, ISC and photochemical reactions, is inefficient. This is an advantage for the design of dyes with significant photostability[47] as the formation of long-lived and potentially reactive excited triplet states is avoided.

In acetonitrile the presence of oxygen has only a marginal effect on the ISC efficiency. However, for toluene solutions, and here especially for the dyes **2**–**4**, a marked increase of Φ_{ISC} value was observed when comparing aerobic and anaerobic conditions (factors of 2–3.5; see Table 1 and Figure 6). This is interpreted in terms of the mechanistic proposal provided in Scheme 2. Namely, we suggest that the interaction of the excited singlet states with oxygen in toluene (by dynamic and static interactions) generates singlet exciplexes[52] that undergo ISC and then finalize in excited triplet states of the dyes. This pathway operates in parallel to the "normal" triplet state generation through ISC of the excited singlet state. This exciplex-

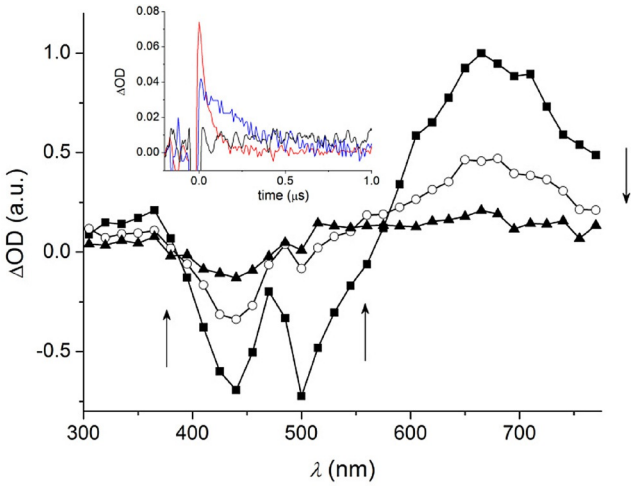

Figure 6. Transient absorption spectrum of **4** in aerated toluene solution; λ_{exc} = 355 nm, time window = 50–600 ns. Inset: The kinetics at 650 nm; black line = N_2-saturated, blue = aerated, red = O_2-saturated. The amplitudes of the kinetic traces reflect the increasing ISC quantum yield in the presence of increasing oxygen concentrations.

© 2018 Wiley-VCH Verlag GmbH & Co. KGaA, Weinheim

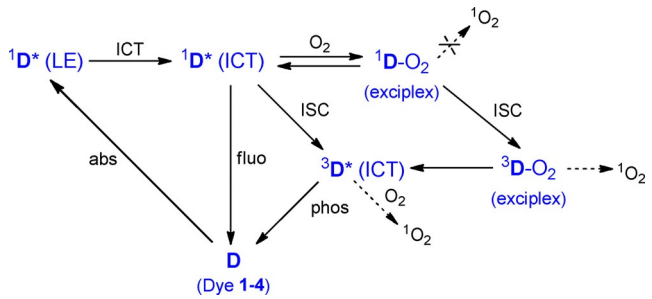

Scheme 2. Proposal for the main excited-state pathways for the dyes **1**–**4** in a non-polar medium (e.g., toluene); abs: absorption, fluo: fluorescence, phos: phosphorescence, ICT: intramolecular charge transfer, ISC: intersystem crossing.

promoted triplet state generation seems especially relevant for the organoboron dyes with strong electron-donating substituents (i.e., in **3** and **4**). Similar observations of oxygen-enhanced ISC have been made for other aromatic chromophores.[53] In accordance with the mechanistic proposal it is not a coincidence that for these dyes also the most relevant contribution of static fluorescence quenching by oxygen, i.e., exciplex formation, was observed (see above).

2.3. Singlet-Oxygen Generation from 1–4

The decay traces of singlet-oxygen phosphorescence at $\lambda =$ 1270 nm generated by pulsed-laser irradiation of aerated toluene solutions of **1**–**4** at 355 nm were recorded. All decays show lifetimes of circa 38 μs. The values of Φ_Δ, obtained with perinaphthenone as reference, are 0.34, 0.09, 0.09, and 0.08 for **1**–**4**, respectively. Especially for the ICT dyes **2**–**4**, these quantum yields are somewhat higher than the corresponding Φ_{ISC} values under anaerobic conditions, which supports the involvement of the postulated exciplex in the generation of singlet oxygen (Scheme 2). However, in general terms the absolute efficiency of this process remains low for **2**–**4**. The direct generation of singlet oxygen from the singlet exciplex is thermodynamically unfavorable since the singlet–triplet energy gap of the dyes **1**–**4** is only 0.4–0.6 eV. This is not sufficient to promote the generation of singlet oxygen, whose energy is 1.0 eV.[54] The inefficient formation of potentially cytotoxic singlet oxygen from the dyes **2**–**4** may be considered an advantage for their use in bioimaging.

3. Conclusions

Four-coordinate N,C-chelate organoboron dyes based on arylisoquinoline ligands with varying electron-donor substitution lead to differentiated photophysical behavior. On the one hand, for **1**, the dye with the least significant ICT character in the investigated series, a smaller fluorescence quantum yield is accompanied by significant triplet state formation and singlet-oxygen production with quantum yields larger than 0.3. On the other hand, the methoxy-substituted **2** and especially the amino-substituted **3** and **4** feature significant ICT character.[47] This mechanism preserves high fluorescence quantum yields and consequently minor triplet state and singlet-oxygen formation ($\leq$0.15 in both cases). An exception is constituted by the IPET fluorescence quenching of **4** in polar solvents, such as acetonitrile. Oxygen quenching of the singlet states is efficient, but has overall a small effect on the fluorescence quantum yields, reasoned with the relatively small fluorescence lifetimes (circa 5–10 ns). Femtosecond transient spectroscopy of dye **4** provided clear proof for the formation of LE and ICT states. Nanosecond laser flash photolysis allowed mainly the detection of the triplet states. The herein obtained mechanistic picture is in accordance with the appropriateness of the dyes for bioimaging applications under aerobic conditions and establishes the ICT mechanism as a beneficial feature for high photostability.[47]

Experimental Section

Chemicals

Compounds **1**–**4** were available from a previous study.[47] Benzophenone, perinaphthenone, and β-carotene (β-C) were purchased from Aldrich in the highest purity available. Spectroscopic grade acetonitrile and toluene were from Scharlau and used without further purification.

Absorption and Emission Measurements

UV/Vis absorption spectra were recorded on a PerkinElmer Lambda 35 spectrophotometer. Fluorescence emission spectra were measured on a Photon Technology International (PTI) LPS-220B fluorimeter. Lifetimes were obtained with a lifetime spectrometer (TimeMaster TM-2/2003 from PTI) by means of the stroboscopic technique. A hydrogen/nitrogen flash lamp (1.8 ns pulse width) was used as excitation source. The kinetic traces were fitted with monoexponential decay functions. Measurements were done under aerobic (air and oxygen) and anaerobic (nitrogen) conditions at room temperature (25 °C) in cuvettes of 1 cm optical path length. The excitation wavelength used to register the fluorescence lifetimes was 375 nm. Quinine bisulfate in 0.5 M H_2SO_4 ($\Phi_{fluo} = 0.546$) was used as standard for the fluorescence quantum yield measurements.[55,56]

The fluorescence quenching rate constants (k_q) by oxygen were determined by using the Stern–Volmer Equation (1) or Equation (2):

$$\Phi_0/\Phi = 1 + k_q \times \tau_0 \times [O_2] \quad (1)$$

$$\tau_0/\tau = 1 + k_q \times \tau_0 \times [O_2] \quad (2)$$

where the index "0" denotes the quantum yield (Φ) or lifetime (τ) in absence of oxygen. Equation (2) allows the determination of the dynamic quenching rate constant. In acetonitrile both equations give the same value for k_q.

For toluene the association constants (K_a) of the dyes with oxygen, corresponding to static fluorescence quenching, were determined with Equation (3):

$$\Phi_0/\Phi = (1 + k_q \times \tau_0 \times [O_2]) \times (1 + K_a \times [O_2]) \quad (3)$$

The radiative decay rate constants (k_r), intersystem crossing (ISC) rate constants (k_{ISC}), and non-radiative decay rate constants (k_{nr}, not

© 2018 Wiley-VCH Verlag GmbH & Co. KGaA, Weinheim

accounting for ISC) for the dyes **1**–**3** and for dye **4** in toluene were calculated with the aid of Equations (4)–(6):

$$k_r = \Phi_{fluo}/\tau_{fluo} \quad (4)$$

$$k_{ISC} = \Phi_{ISC}/\tau_{fluo} \quad (5)$$

$$k_{nr} = (1-\Phi_{fluo}-\Phi_{ISC})/\tau_{fluo} \quad (6)$$

For dye **4** in acetonitrile the IPET rate constant was determined by Equation (7), assuming that IPET is the only excited-state decay pathway that competes with fluorescence:

$$k_{IPET} = (1-\Phi_{fluo})/\tau_{fluo} \quad (7)$$

Phosphorescence measurements in toluene at 77 K were done with a lifetime spectrometer (TimeMaster TM-2/2003 from PTI), equipped with a single-cell Peltier cooler. The emission spectral band widths were set to 5 nm at 420 nm excitation wavelength. The phosphorescence emission spectra were taken with a delay time of 0.5 ms and a total gate time of 10 ms. The triplet excitation energies of compounds were calculated from the onset of the phosphorescence spectrum.

The singlet excitation energies in toluene were calculated by averaging the energies corresponding to the long-wavelength absorption maximum[47] and the emission maximum, according to a published procedure.[57]

Nanosecond Laser Flash Photolysis Experiments

A pulsed Nd:YAG laser was used at 355 nm. The single pulses were of circa 10 ns duration and the energy was from 10 to 1 mJ per pulse. The laser flash photolysis apparatus consisted of the pulsed laser, a pulsed xenon lamp as detecting light source, a monochromator, and a photomultiplier. The output signal from the oscilloscope was transferred to a personal computer.

The transient spectra of compound **1**–**4** were recorded in organic solvents (toluene or acetonitrile) using 10×10 mm^2 quartz cells with 3 mL capacity. Saturation of the solutions with oxygen or nitrogen was achieved by bubbling during 20 min with the respective gas. The absorbance of the samples was kept at circa 0.3 at the excitation laser wavelength (355 nm). The experiments were carried out at room temperature and each measurement was done in triplicate, using freshly prepared samples.

The molar absorption coefficient of triplet state of **1** (^{3}**1***) in toluene was estimated by monitoring the energy transfer reaction between ^{3}**1*** and β-C. The study was performed with N_2-saturated toluene solutions of **1** in the presence of β-C (5×10^{-5}–2×10^{-4} M) using a 355 nm laser pulse. The molar absorption coefficient (ε) of ^{3}**1*** at 640 nm was calculated by concomitant monitoring of the triplet–triplet absorption signal of ^{3}β-C* at 525 nm and using Equations (8) and Equation (9):[58]

$$\Delta A(^3\beta\text{-C}^*, 525\,nm) = \Delta A(^3\beta\text{-C}^*, 525\,nm)_{max} \times \exp[\ln(k_3/k_2)/(1-k_2/k_3)] \quad (8)$$

$$\varepsilon(^3\mathbf{1}^*, 640\,nm) = \Delta A(^3\mathbf{1}^*, 640\,nm) \times \varepsilon(^3\beta\text{-C}^*, 525\,nm) \times ((k_2-k_1)/k_2)/\Delta A(^3\beta\text{-C}^*, 525\,nm) \quad (9)$$

$\Delta A(^3\beta$-C*, 525 nm) was determined from Equation (8), because the decay rate constant of $^3\beta$-C* (k_3) is not small compared with the ^{3}**1*** decay rate constant (k_2) obtained at the different concentrations of β-C. $\Delta A(^3\beta\text{-C}^*, 525\,nm)_{max}$ refers to the maximum absorption detected for $^3\beta$-C* at 525 nm. In Equation (9) $\Delta A(^3$**1***, 640 nm) is the absorbance change of ^{3}**1*** at 640 nm immediately after the laser flash and k_1 is the decay rate constant of ^{3}**1*** in absence of β-C. The molar absorption coefficient for $^3\beta$-C* in toluene at 525 nm was taken as 119000 M^{-1} cm^{-1}.[59]

The intersystem crossing (ISC) quantum yields (Φ_{ISC}) were obtained by a comparative method[58] assuming that the molar absorption coefficient of the excited triplet state is similar for all investigated organoboron dyes. As reference optically matched benzophenone (BP) solutions (0.3 at 355 nm) were used and Equation (10) was applied:

$$\Phi_{ISC}(\mathbf{1}-\mathbf{4}) = \Phi_{ISC}(BP) \times \Delta A(\mathbf{1}-\mathbf{4}, 640\,nm) \times \varepsilon(^3BP^*, 525\,nm)/(\Delta A(^3BP^*, 525\,nm) \times \varepsilon(\mathbf{1}-\mathbf{4}, 640\,nm)) \quad (10)$$

where the ΔA values refer to the absorbance of the triplet-excited organoboron dyes at 640 nm and to ^{3}BP* at 525 nm. The molar absorption coefficient of triplet-excited benzophenone [$\varepsilon(^3$BP*, 525 nm)] and its intersystem quantum yield [Φ_{ISC}(BP)] in acetonitrile were taken as 6500 M^{-1} cm^{-1} and 1, respectively, and assumed to be the same in toluene.[60]

The triplet quenching rate constants by oxygen (k_q) were determined using Equation (11):

$$1/\tau_T = 1/\tau_{T,0} + k_q[O_2] \quad (11)$$

Femtosecond Transient Absorption Spectroscopy

Transient absorption spectra were recorded using a typical pump–probe setup. The femtosecond pulses were generated with a compact regenerative amplifier that produces pulses centered at 800 nm (circa 100 fs, 1 mJ per pulse). The output of the laser was split into two parts to generate the pump and the probe beams. Thus, tuneable femtosecond pump pulses were obtained by directing the 800 nm light into an optical parametric amplifier. In the present case, the pump was set at 350 nm and passed through a chopper prior to focusing onto a rotating cell (0.8 mm optical path length) containing the sample solution. The white light used as probe was produced after part of the 800 nm light from the amplifier passed through a computer-controlled 8 ns variable optical delay line and impinged on a CaF_2 rotating crystal. This white light was split in two identical portions to generate reference and probe beams that then were focused on the rotating cell containing the sample. The pump and the probe coincided in the interrogation of the sample. A computer-controlled imaging spectrometer was placed after this path to measure the probe and the reference pulses and to obtain the transient absorption decays and spectra.

Singlet Oxygen Measurements

The singlet-oxygen phosphorescence decay traces after the laser pulse were registered at 1270 nm employing a Peltier-cooled (−62.8 °C) Hamamatsu NIR detector operating at 650 V, coupled to a computer-controlled grating monochromator. A pulsed Nd:YAG L52137 V LOTIS TII was used at the excitation wavelength of 355 nm. The single pulses were of circa 10 ns duration, and the energy was lower than 5 mJ per pulse. The system consisted of the

© 2018 Wiley-VCH Verlag GmbH & Co. KGaA, Weinheim

pulsed laser, a 77250 Oriel monochromator coupled to the Hamamatsu NIR detector and the oscilloscope connected to the computer. The output signal was transferred from the oscilloscope to a personal computer. All measurements were made at room temperature, under an air atmosphere, and using toluene as solvent in 10×10 mm^2 quartz cells with a capacity of 4 mL. The absorbance of the samples was 0.30 at the laser excitation wavelength. The singlet-oxygen quantum yield (Φ_Δ) was determined for each compound using perinaphthenone in toluene ($\Phi_\Delta=0.97$) as reference.[61] The singlet-oxygen quantum yield [Eq. (12)] was calculated from the slope m of the plots of the phosphorescence signal intensity directly after the laser pulse versus the laser light intensity, using a set of neutral density filters to vary the laser intensity.

$$\Phi_\Delta(\mathbf{1-4}) = \Phi_{\Delta(\text{perinaphthenone})} \times m(\mathbf{1-4})/m_{(\text{perinaphthenone})} \qquad (12)$$

Acknowledgements

The funding by the Spanish Ministry of Economy, Industry, and Competitiveness (grants CTQ2014-54729-C2-1-P for U.P., CTQ2014-54729-C2-2-P for F.B., CTQ2013-48164-C2-1-P, CTQ2013-48164-C2-2-P for A.R., Ramon y Cajal contract RYC-2013–12585 for A.R.), the European Union (ERDF), the Andalusian Government (grants 2012/FQM-2140 for U.P., 2009/FQM-4537 and 2012/FQM-1078 for A.R.), and the University of Huelva (postdoctoral contract for V.F.P.) is gratefully acknowledged.

Keywords: charge transfer · fluorescence · organoboron dyes · photophysics · singlet oxygen

[1] M. Elbing, G. C. Bazan, *Angew. Chem. Int. Ed.* **2008**, *47*, 834 – 838; *Angew. Chem.* **2008**, *120*, 846 – 850.
[2] L. Ji, S. Griesbeck, T. B. Marder, *Chem. Sci.* **2017**, *8*, 846 – 863.
[3] C.-H. Zhao, A. Wakamiya, Y. Inukai, S. Yamaguchi, *J. Am. Chem. Soc.* **2006**, *128*, 15934 – 15935.
[4] D.-R. Bai, X.-Y. Liu, S. Wang, *Chem. Eur. J.* **2007**, *13*, 5713 – 5723.
[5] A. Proń, G. Zhou, H. Norouzi-Arasi, M. Baumgarten, K. Müllen, *Org. Lett.* **2009**, *11*, 3550 – 3553.
[6] H. Pan, G.-L. Fu, Y.-H. Zhao, C.-H. Zhao, *Org. Lett.* **2011**, *13*, 4830 – 4833.
[7] A. G. Bonn, O. S. Wenger, *J. Org. Chem.* **2015**, *80*, 4097 – 4107.
[8] Z.-Q. Liu, Q. Fang, D.-X. Cao, D. Wang, G.-B. Xu, *Org. Lett.* **2004**, *6*, 2933 – 2936.
[9] P. Chen, A. S. Marshall, S.-H. Chi, X. Yin, J. W. Perry, F. Jäkle, *Chem. Eur. J.* **2015**, *21*, 18237 – 18247.
[10] Y. Kubo, M. Yamamoto, M. Ikeda, M. Takeuchi, S. Shinkai, S. Yamaguchi, K. Tamao, *Angew. Chem. Int. Ed.* **2003**, *42*, 2036 – 2040; *Angew. Chem.* **2003**, *115*, 2082 – 2086.
[11] M. Melaimi, F. P. Gabbaï, *J. Am. Chem. Soc.* **2005**, *127*, 9680 – 9681.
[12] T. W. Hudnall, Y.-M. Kim, M. W. P. Bebbington, D. Bourissou, F. P. Gabbaï, *J. Am. Chem. Soc.* **2008**, *130*, 10890 – 10891.
[13] C. R. Wade, A. E. J. Broomsgrove, S. Aldridge, F. P. Gabbaï, *Chem. Rev.* **2010**, *110*, 3958 – 3984.
[14] Z. M. Hudson, X.-Y. Liu, S. Wang, *Org. Lett.* **2011**, *13*, 300 – 303.
[15] S. Griesbeck, Z. Zhang, M. Gutmann, T. Lühmann, R. M. Edkins, G. Clermont, A. N. Lazar, M. Haehnel, K. Edkins, A. Eichhorn, M. Blanchard-Desce, L. Meinel, T. B. Marder, *Chem. Eur. J.* **2016**, *22*, 14701 – 14706.
[16] Y.-L. Rao, S. Wang, *Inorg. Chem.* **2011**, *50*, 12263 – 12274.
[17] D. Li, H. Zhang, Y. Wang, *Chem. Soc. Rev.* **2013**, *42*, 8416 – 8433.
[18] Y.-L. Rao, H. Amarne, S.-B. Zhao, T. M. McCormick, S. Martić, Y. Sun, R.-Y. Wang, S. Wang, *J. Am. Chem. Soc.* **2008**, *130*, 12898 – 12900.
[19] H. Amarne, C. Baik, S. K. Murphy, S. Wang, *Chem. Eur. J.* **2010**, *16*, 4750 – 4761.
[20] S. K. Mellerup, K. Yuan, C. Nguyen, Z.-H. Lu, S. Wang, *Chem. Eur. J.* **2016**, *22*, 12464 – 12472.
[21] A. Coskun, E. U. Akkaya, *J. Am. Chem. Soc.* **2006**, *128*, 14474 – 14475.
[22] S. O. McDonnell, D. F. O'Shea, *Org. Lett.* **2006**, *8*, 3493 – 3496.
[23] A. Loudet, K. Burgess, *Chem. Rev.* **2007**, *107*, 4891 – 4932.
[24] G. Ulrich, R. Ziessel, A. Harriman, *Angew. Chem. Int. Ed.* **2008**, *47*, 1184 – 1201; *Angew. Chem.* **2008**, *120*, 1202 – 1219.
[25] Q. Zheng, G. Xu, P. N. Prasad, *Chem. Eur. J.* **2008**, *14*, 5812 – 5819.
[26] J. Han, A. Loudet, R. Barhoumi, R. C. Burghardt, K. Burgess, *J. Am. Chem. Soc.* **2009**, *131*, 1642 – 1643.
[27] O. A. Bozdemir, R. Guliyev, O. Buyukcakir, S. Selcuk, S. Kolemen, G. Gulseren, T. Nalbantoglu, H. Boyaci, E. U. Akkaya, *J. Am. Chem. Soc.* **2010**, *132*, 8029 – 8036.
[28] D. Frath, S. Azizi, G. Ulrich, P. Retailleau, R. Ziessel, *Org. Lett.* **2011**, *13*, 3414 – 3417.
[29] L.-Y. Niu, Y.-S. Guan, Y.-Z. Chen, L.-Z. Wu, C.-H. Tung, Q.-Z. Yang, *J. Am. Chem. Soc.* **2012**, *134*, 18928 – 18931.
[30] D. Frath, A. Poirel, G. Ulrich, A. De Nicola, R. Ziessel, *Chem. Commun.* **2013**, *49*, 4908 – 4910.
[31] S. Erbas-Cakmak, O. A. Bozdemir, Y. Cakmak, E. U. Akkaya, *Chem. Sci.* **2013**, *4*, 858 – 862.
[32] S. Zhang, T. Wu, J. Fan, Z. Li, N. Jiang, J. Wang, B. Dou, S. Sun, F. Song, X. Peng, *Org. Biomol. Chem.* **2013**, *11*, 555 – 558.
[33] X. Zhang, Y. Xiao, J. Qi, J. Qu, B. Kim, X. Yue, K. D. Belfield, *J. Org. Chem.* **2013**, *78*, 9153 – 9160.
[34] D. Frath, J. Massue, G. Ulrich, R. Ziessel, *Angew. Chem. Int. Ed.* **2014**, *53*, 2290 – 2310; *Angew. Chem.* **2014**, *126*, 2322 – 2342.
[35] H. Lu, J. Mack, Y. Yang, Z. Shen, *Chem. Soc. Rev.* **2014**, *43*, 4778 – 4823.
[36] D. Collado, Y. Vida, F. Nájera, E. Pérez-Inestrosa, *RSC Adv.* **2014**, *4*, 2306 – 2309.
[37] T. Kowada, H. Maeda, K. Kikuchi, *Chem. Soc. Rev.* **2015**, *44*, 4953 – 4972.
[38] S. Kolemen, M. Işık, G. M. Kim, D. Kim, H. Geng, M. Buyuktemiz, T. Karatas, X.-F. Zhang, Y. Dede, J. Yoon, E. U. Akkaya, *Angew. Chem. Int. Ed.* **2015**, *54*, 5340 – 5344; *Angew. Chem.* **2015**, *127*, 5430 – 5434.
[39] S. P. J. T. Bachollet, D. Volz, B. Fiser, S. Münch, F. Rönicke, J. Carrillo, H. Adams, U. Schepers, E. Gómez-Bengoa, S. Bräse, J. P. A. Harrity, *Chem. Eur. J.* **2016**, *22*, 12430 – 12438.
[40] F. M. F. Santos, J. N. Rosa, N. R. Candeias, C. Parente Carvalho, A. I. Matos, A. E. Ventura, H. F. Florindo, L. C. Silva, U. Pischel, P. M. P. Gois, *Chem. Eur. J.* **2016**, *22*, 1631 – 1637.
[41] J. Wang, Q. Wu, C. Yu, Y. Wei, X. Mu, E. Hao, L. Jiao, *J. Org. Chem.* **2016**, *81*, 11316 – 11323.
[42] J. H. Golden, J. W. Facendola, D. M. R. Sylvinson, C. Quintana Baez, P. I. Djurovich, M. E. Thompson, *J. Org. Chem.* **2017**, *82*, 7215 – 7222.
[43] M. Urban, K. Durka, P. Jankowski, J. Serwatowski, S. Luliński, *J. Org. Chem.* **2017**, *82*, 8234 – 8241.
[44] D. Frath, P. Didier, Y. Mély, J. Massue, G. Ulrich, *ChemPhotoChem* **2017**, *1*, 109 – 112.
[45] M. M. Alcaide, F. M. F. Santos, V. F. Pais, J. I. Carvalho, D. Collado, E. Pérez-Inestrosa, J. F. Arteaga, F. Boscá, P. M. P. Gois, U. Pischel, *J. Org. Chem.* **2017**, *82*, 7151 – 7158.
[46] V. F. Pais, J. M. Lassaletta, R. Fernández, H. S. El-Sheshtawy, A. Ros, U. Pischel, *Chem. Eur. J.* **2014**, *20*, 7638 – 7645.
[47] V. F. Pais, M. M. Alcaide, R. López-Rodríguez, D. Collado, F. Nájera, E. Pérez-Inestrosa, E. Álvarez, J. M. Lassaletta, R. Fernández, A. Ros, U. Pischel, *Chem. Eur. J.* **2015**, *21*, 15369 – 15376.
[48] V. F. Pais, P. Ramírez-López, A. Romero-Arenas, D. Collado, F. Nájera, E. Pérez-Inestrosa, R. Fernández, J. M. Lassaletta, A. Ros, U. Pischel, *J. Org. Chem.* **2016**, *81*, 9605 – 9611.
[49] R. Bensasson, E. J. Land, B. Maudinas, *Photochem. Photobiol.* **1976**, *23*, 189 – 193.
[50] R. F. Dallinger, W. H. Woodruff, M. A. J. Rodgers, *Photochem. Photobiol.* **1981**, *33*, 275 – 277.
[51] B. R. Nielsen, K. Jørgensen, L. H. Skibsted, *J. Photochem. Photobiol. A* **1998**, *112*, 127 – 133.
[52] S. L. Logunov, M. A. J. Rodgers, *J. Phys. Chem.* **1992**, *96*, 2915 – 2917.
[53] R. Schmidt, *Photochem. Photobiol.* **2006**, *82*, 1161 – 1177.
[54] A. A. Krasnovskiĭ, *Biofizika* **1976**, *21*, 748 – 749.
[55] W. H. Melhuish, *J. Phys. Chem.* **1960**, *64*, 762 – 764.
[56] W. H. Melhuish, *J. Phys. Chem.* **1961**, *65*, 229 – 235.
[57] S. R. Greenfield, W. A. Svec, D. Gosztola, M. R. Wasielewski, *J. Am. Chem. Soc.* **1996**, *118*, 6767 – 6777.
[58] I. Carmichael, G. L. Hug, *J. Phys. Chem. Ref. Data* **1986**, *15*, 1 – 250.

© 2018 Wiley-VCH Verlag GmbH & Co. KGaA, Weinheim

[59] J. N. Silva, F. Boscá, J. P. C. Tomé, E. M. P. Silva, M. G. P. M. S. Neves, J. A. S. Cavaleiro, L. K. Patterson, P. Filipe, J. C. Mazière, R. Santus, P. Morlière, *J. Phys. Chem. B* **2009**, *113*, 16695 – 16704.
[60] R. V. Bensasson, J.-C. Gramain, *J. Chem. Soc. Faraday Trans. 1* **1980**, *76*, 1801 – 1810.
[61] C. Grewer, H. D. Brauer, *J. Phys. Chem.* **1993**, *97*, 5001 – 5006.

Manuscript received: October 4, 2017
Revised manuscript received: November 23, 2017
Version of record online: December 8, 2017

© 2018 Wiley-VCH Verlag GmbH & Co. KGaA, Weinheim